

Available online at www.sciencedirect.com**ScienceDirect**

Energy Procedia 55 (2014) 643 – 648

Energy

Procedia

4th International Conference on Silicon Photovoltaics, SiliconPV 2014

Improvement on industrial n-type bifacial solar cell with >20.6% efficiency

Hung-Chih Chang^a, Chih-Jeng Huang^a, Po-Tsung Hsieh^{a*}, Wei-Cheng Mo^a,
Shu-Hung Yu^a, Chi-Chun Li^a

^a*Motech Industries, Inc. Science Park Branch, 74145 Tainan, Taiwan*

Abstract

Results of industrial n-type bifacial solar cells, with efficiency as high as 20.63%, are presented within this work. 6" n-Cz wafers were used as substrates. The front emitter and the back surface field were fabricated by boron and phosphorous diffusions respectively. Various surface structures and doping conditions were adopted for comparisons for their influence on cell performance. In addition, three Ag/Al pastes were tested and their related properties were discussed. With the integration of these improved processes, better electrical properties, including higher cell efficiency were obtained.

© 2014 Published by Elsevier Ltd. This is an open access article under the CC BY-NC-ND license (<http://creativecommons.org/licenses/by-nc-nd/3.0/>).

Peer-review under responsibility of the scientific committee of the SiliconPV 2014 conference

Keywords: n-type, bifacial, boron doping, texture.

1. Introduction

As is well known, a sizable reduction in performance of industrial p-type Si solar cells takes place after the cells are exposed to light. This light induced degradation (LID) effect has been shown to result from the boron-oxygen complex in the p-type Si wafer [1-3]. The doped boron atoms react with oxygen atoms under illumination, forming B-O complexes that degrade the bulk lifetime of Si wafer [4-6]. As such, one major approach to avoid LID is to use wafers without boron doping, and the most readily available option is the n-type Si material. Additional advantages of n-type wafers include longer minority carrier diffusion length and less sensitivity to metallic impurities [7]. A few

* Corresponding author. Tel.: +886-6-5050789ext.0643; fax: +886-6-5058446.

E-mail address: potsung_hsieh@motech.com.tw

products using n-type Si substrates have been available, including interdigitated back-contact (IBC) cells from SunPower, and heterojunction with intrinsic thin layer (HIT) cells from Panasonic [8, 9]. Though much effort has been made to develop various n-type cell structures with high efficiency, the cost often increased significantly due to additional processing steps. Bifacial n-type cell structure holds the potential for both achieving high efficiency and keeping the production cost low, by utilizing industrial production processes. A number of institutions have reported high efficiency values of n-type bifacial cells, including Motech's 20.23% announced last year [10-11]. In this work, an improvement to 20.63% cell efficiency is presented. The effect of different surface structures and doping conditions are discussed. Furthermore, three different Ag/Al pastes were applied to the bifacial n-type cells to compare their electrical performance.

2. Experiment

In this study, 6-inch n-type Cz silicon wafers with an initial thickness of 180 μm were used. After texturing, the wafers were then doped with boron for front emitter, and with phosphorous for back surface field. Passivation films and SiN_x ARC films were deposited on the doped surfaces. Front-side and back-side metallization were completed by screen-printing Ag/Al and Ag pastes respectively. Schematic cross section of N-type bifacial cell structure is shown in Fig. 1. Several processes improvement were addressed and investigated based on previous study [5, 6].

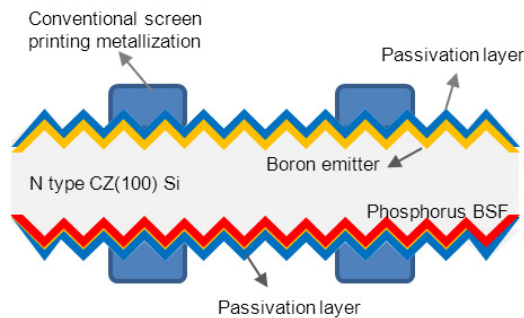


Fig. 1. Schematic cross-section of N-type bifacial solar cell.

3. Results and discussion

Figure 2 compares the electrical results of bifacial cells with three different rear side textures, TX1, TX2, and TX3. TX1 is the original texturing process. In order to reduce the surface recombination, additional smoothening processes were applied on TX2 and TX3. Longer process time was used on TX3 than TX2, which means the surface of TX3 should be smoother than TX2. As shown in the Fig. 2, higher open circuit voltage (V_{oc}) was obtained by adopting TX2 and TX3. Relative 0.6% gain can be observed for TX3 process. Improvement in short circuit current (I_{sc}) can also be obtained by TX2 and TX3, as compared to TX1. Over 1% relative gain was measured for TX3 sample. As shown in Fig. 3, the surface morphology of TX3 is smoother than textured surface, which is beneficial for V_{oc} and I_{sc} . Cell efficiency gain was over 3% gain, due to enhanced V_{oc} , I_{sc} , and also the fill factor (FF). As illustrated in the right figure of Fig. 2, series resistances (R_s) for TX2 and TX3 were lower than TX1, which resulted in FF gain. Comparing TX2 and TX3: TX2 exhibited lower R_s than TX3, which indicated better suitability of TX2 for metallization. However, FF remains the same for TX2 and TX3 as indicated in the figure. Using SunsVoc measurement we found that the pseudo fill factor (PFF) of TX3 was higher than that of TX2, which compensated the difference in R_s , and resulted in comparable FF for TX2 and TX3.



Fig. 2. Comparison of I-V parameters of rear side texturing processes. Changes relative to TX1 are shown.

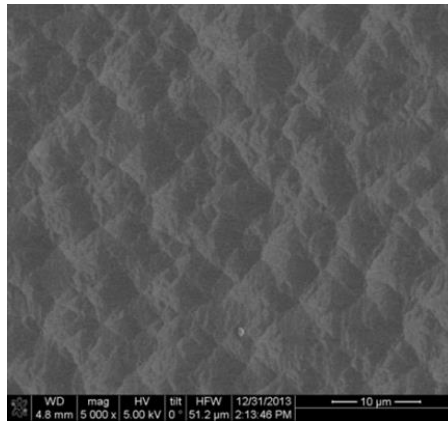


Fig. 3. Morphology of rear side surface.

Boron doping is always a critical process for n-type cell for the formation of emitter layer. In order to evaluate boron doping quality, a symmetrical structure for QSSPC measurement was prepared. Figure 4 shows the emitter saturation current density (J_0) and effective lifetime (T_{eff}) for different boron doping recipes (P1, P2 and P3). It is well-known that higher process temperature is always needed for boron diffusion than phosphorous diffusion based on different doping mechanism for boron and phosphorous atoms to Si surface. However, it is also important to control the thickness of boron rich layer during diffusion process. Therefore, the process adjustments from P1 to P3 are mainly on thermal budget, with P3 having the least thermal budget. It depicts that J_0 and T_{eff} were improved during the optimization, P1 to P2 to P3, indicating less surface recombination and defect for P3 compared to P1 and P2. Figure 5 presents the relative cell IV results. P1 is the original baseline and serves as the base of comparison. Higher Voc values were measured with P2 and P3 conditions, consistent with the QSSPC results. Nearly 2% of relative gain on Voc can be achieved with P3. In addition to Voc, it is worth mentioning that Rs was also reduced for P2 and P3 (not shown here). Due to the improvement on Rs, FF increased by 4% relative. As a result, better cell efficiency performance was observed by using P3 recipe with the enhanced Voc, Jsc and FF.

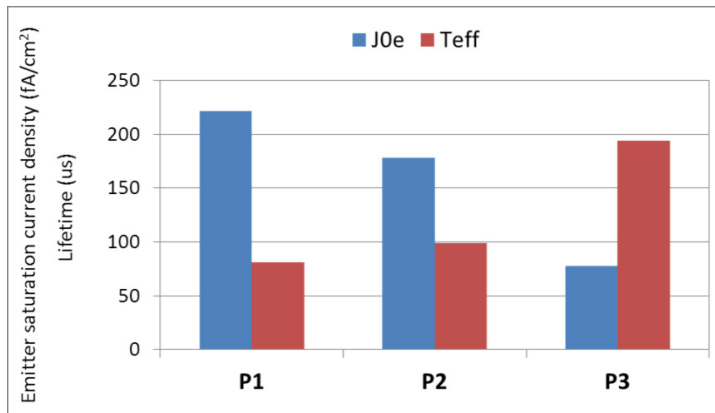


Fig. 4. Measured Joe and Teff as functions of various boron diffusion parameters.

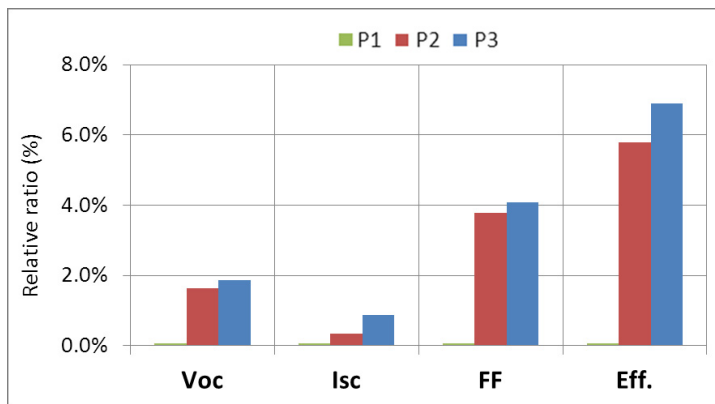


Fig. 5. Relative I-V results for various boron diffusion parameters.

Front Ag/Al paste for boron emitter plays a crucial role in n-type bifacial solar cells. Fig. 6 shows the comparison of relative I-V values for the three Ag/Al pastes we tested and Figure 7 presents the comparisons on R_s and printed finger width for various pastes. Due to different paste compositions and viscosities, wider finger width was obtained with Paste A than the other two pastes using the same screen opening, and thus resulted in lower I_{sc} for Paste A. Similar I_{sc} results were observed for Paste B and Paste C due to similar metal finger widths. Figure 8 shows the image of printed finger by Paste C and less spread at sidewall of the finger was observed. Lower V_{oc} for Paste B than Paste C could be ascribed to different Al content of pastes. As compared with Figure 6 and Figure 7, better fill factor obtained by Paste C resulted from the lower R_s . According to Transmission Line Measurement results (not shown here), Paste C exhibited the lowest contact resistance. Based on the results above, Paste C has better performance not only in I_{sc} and V_{oc} , but also in FF. The highest cell efficiency was obtained by Paste C.

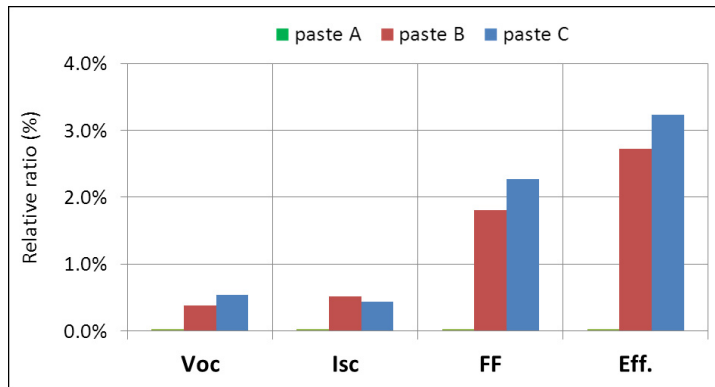


Fig. 6. I-V results for various pastes. Changes relative to Paste A are shown.

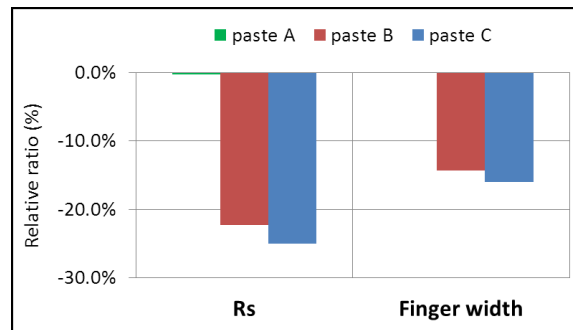


Fig. 7. Comparison on Rs (series resistance) and printed finger width for various pastes.

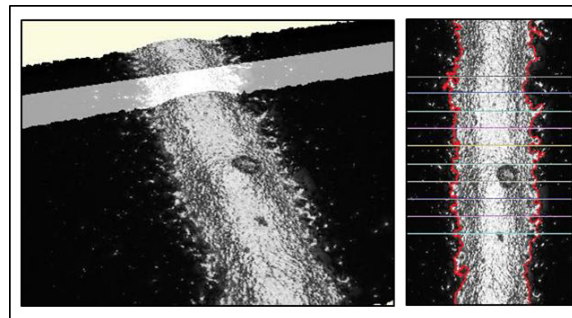


Fig. 8 Photos for printed finger by paste C.

Integrating the optimized processes discussed above, we were able to produce a bifacial cell with efficiency reaching 20.63%. Table 1 shows the basic electrical data of the best cell.

Table 1. I-V characteristics of the champion cell.

Chuck type	Voc (mV)	Jsc (mA/cm ²)	FF (%)	Eff. (%)
Metal coated chuck (ITRI_SCCL)	647	39.2	81.3	20.63

4. Conclusion

Efficiency up to 20.63% for N-type bifacial solar cells was achieved by industrial processes. Investigations on rear surface texture formation, boron doping conditions and various metal pastes showed significant influence on Voc, Isc and FF. Results indicate that higher cell efficiency is reachable with optimized cell structure, and continued improvement in processes.

Acknowledgements

The authors would like to thank Solar cell Calibration and Characterization Laboratory (SCCL) of Taiwan's Industrial Technology Research Institute (ITRI) for providing platform of solar cell efficiency measurement.

References

- [1] D. Song, J. Xiong, Z. Hu, G. Li, H. Wang, H. An, B. Yu, B. Grenko, K. Borden, K. Sauer, T. Roessler, J. Cui, H. Wang, J. Bultman, A. H. G. Vlooswijk and P. R. Venema, IEEE 38th Photovoltaic Specialists Conference, 2012.
- [2] T. S. Böske, D. Kania, A. Helbig, T. Roth, C. Schöllhorn, M. Dupke, P. Sadler, M. Braun, D. Stichtenoth, T. Wütherich, R. Jesswein, D. Fiedler, R. Carl, J. Lossen, and H. J. Krokoszinski, IEEE Journal of Photovoltaics, vol PP, issue 99, 2013, p.1.
- [3] J. Schmidt and R. Hezel, 12th Workshop on Crystalline Silicon Solar Cell Materials and Processes, 2002.
- [4] J. Schmidt, A. G. Aberle and R. Hezel, 26th IEEE Photovoltaic Specialist Conference, 1997, p.13.
- [5] A. Mohr, P. Engelhart, C. Klenke, S. Wanka, A. A. Stekolnikov, M. Scherff, R. Sequin, S. Tardon, T. Ridolph, M. Hofmann, F. Stenzel, J. Lee, S. Diez, J. Wendt, W. Brendle, S. Schmidt, J. W. Müller, P. Wawer, M. Hhofmann, P. Saint-Cast, J. Nekarda, D. Erath, J. Rentsch, R. Preu, Proceedings of the 26th European Photovoltaic Solar Energy Conference, 2011, p.15591.
- [6] I. Romijn, Photovoltaics International Edition 15, 2012, p.81.
- [7] D. Macdonald and L. J. Geerligs, Appl. Phys. Lett., 85 (2004) 4061-4063.
- [8] P. J. Cousins, D. D. Smith, H. C. Luan, J. Manning, T. D. Dennis, A. Waldhauer, K. E. Wilson, G. Harley, G. P. Mulligan, 36th IEEE Photovoltaic Specialist Conference, 2010, p.823.
- [9] T. Kinoshita, D. Fujishima, A. Yano, A. Ogane, S. Tohoda, K. Matsuyama, Y. Nakamura, N. Tokuoka, H. Kanno, H. Sakata, M. Taguchi, E. Maruyama, 26th European Photovoltaic Solar Energy Conference, 2011, p.871.
- [10] P. T. Hsieh, C. J. Huang, H. C. Chang, S. W. Chiu and C. C. Li, 28th European Photovoltaic Solar Energy Conference, 2013.
- [11] P. T. Hsieh, C. J. Huang, H. C. Chang, S. W. Chiu and C. C. Li, 23th Photovoltaic Science and Engineering Conference, 2013.